

## <sup>13</sup>C NMR Analysis of Soot Produced from Model Compounds and a Coal

Mark S. Solum, Adel F. Sarofim, Ronald J. Pugmire,\* Thomas H. Fletcher,<sup>†</sup> and Haifeng Zhang<sup>†</sup>

Department of Chemical and Fuels Engineering, University of Utah, Salt Lake City, Utah 84112, and Department of Chemical Engineering, Brigham Young University, Provo, Utah 84602

Received February 8, 2001. Revised Manuscript Received April 30, 2001

Soot samples, including the associated organics, produced from an Illinois No. 6 coal (five samples) and two model compounds, biphenyl (three samples) and pyrene (two samples), have been studied by <sup>13</sup>C NMR methods. The coal soot data served as a guide to selection of the temperature range that would be most fruitful for investigation of the evolution of aerosols composed of soot and tars that are generated from model compounds. The evolution of the different materials in the gas phase followed different paths. The coal derived soots exhibited loss of aliphatic and oxygen functional groups prior to significant growth in average aromatic cluster size. Between 1410 and 1530 K, line broadening occurs in the aromatic band, which appears to have a Lorentzian component that is observable at the lower temperature and is quite pronounced at the higher temperature. The data indicate that the average aromatic cluster size (the number of carbon atoms in an aromatic ring system where the rings are connected through aromatic bridgehead carbon atoms) may be as large as 80–90 carbons/cluster. The data obtained for the biphenyl samples exhibit a different path for pyrolysis and soot growth. A significant amount of ring opening reactions occurs, followed by major structural rearrangements, after the initial ring opening and hydrogen transfer phase. The cluster size not only grows significantly, but the cross-linking structure also increases, indicating that soot growth in biphenyl soots consists not only of cluster size growth but also cluster cross-linking. The evolution of pyrene aerosol samples follows still another path. Little evidence is noted for ring opening reactions. Major ring growth has not occurred at 1410 K but cross-linking reactions are noted, indicating the formation of dimer/trimer structures. Although a significant amount of ring growth is noted, the data are inconclusive regarding the mechanism for ring growth in the pyrene aerosols between 1410 and 1460 K.

### Introduction

Soot is formed both by pyrolysis and incomplete combustion of fuels. In addition to soot, a wide variety of hydrocarbons are formed in these processes. Soot particles are important in certain industrial applications where intermediate formation of soot is desired to enhance radiative heat transfer. The chemical pathway for soot formation is also applicable to the synthesis of carbon black, valuable in a number of products such as filler material for tires, toner for copiers, etc. The study of the chemical structure/components of soot is also of importance for many environmental reasons as it arises from the condensation of polyaromatic hydrocarbons (PAH) that are formed from a variety of complex mechanisms involving reactive intermediates produced in pyrolysis or combustion processes. Some of these PAHs are known to be carcinogenic, are adsorbed on soots and other ambient aerosols, and may be harmful if inhaled, especially if the aerosol particles are smaller than 2.5 μm.<sup>1–3</sup> Therefore, the study of soot formation has become a topic of substantial interest.

“Soot formation encompasses chemically and physically different processes, e.g., the formation and growth of large aromatic hydrocarbons and their transition to particles, the coagulation of primary particles to larger aggregates, and the growth of solid particles by picking up growth components from the gas phase”.<sup>4</sup> The largest uncertainty in the soot formation mechanisms proposed by different investigators is the gas-to-particle conversion step. Warnatz<sup>5</sup> proposed a detailed mechanism of approximately 250 reactions in the formation of benzene from simple fuels. Frenklach and Warnatz<sup>6</sup> provided mechanisms for the growth of benzene to small PAH's and Frenklach<sup>7</sup> assumed that the further growth of PAH's occurs by polymerization processes. Frenklach<sup>8</sup>

(2) Schwartz, J.; Norris, G.; Larson, T. *Environ. Health Perspect.* **1999**, *107*, 339.

(3) Schwartz, J.; Leas, L. M. *Epidemiology* **2000**, *11*, 6.

(4) Bockhorn, H. In *Soot Formation in Combustion*; Bockhorn, H., Ed.; Springer-Verlag: New York, 1994; p 4.

(5) Warnatz, J.; Chevalier, C. In *Combustion Chemistry*, 2nd ed.; Gardiner, W. C., Jr., Ed.; Springer-Verlag: New York, 1994.

(6) Frenklach, M.; Warnatz, J. *Combust. Sci. Technol.* **1987**, *51*, 265.

(7) Frenklach, M. *Chem. Eng. Sci.* **1985**, *40*, 1843.

(8) Frenklach, M. *Twenty Sixth Symposium (International) on Combustion*; The Combustion Institute: 1996; p 2285.

<sup>†</sup> Department of Chemical Engineering.

(1) Peters, A. *Am. J. Respir. Crit. Care Med.* **1997**, *155*, 1376.

has reported theoretical studies that describe surface growth of soot particles based on the formation of five-member rings that serve as surface nuclei for subsequent HACA (hydrogen abstraction and acetylene addition) growth.

Although the acetylene addition pathway of soot formation is a major one, there is increasing support for polymerization pathways.<sup>9–16</sup> The acetylene addition and polymerization routes for soot formation probably occur in parallel in relative amounts that depend on the fuel and the combustion conditions. To help resolve the pathway to soot formation, it is important to characterize the soot precursors. Mass spectrometry in combination with molecular beam sampling from flames<sup>16–19</sup> and in combination with gas chromatography, high performance liquid chromatography, or laser ablation methods have been used to determine the soot precursors, and in the case of LAMMA,<sup>20</sup> some of the moieties in the soot. The present paper is intended to show the utility of NMR for this purpose. In this paper we will focus on unextracted soot samples to try to identify some of the pathways of formation of soot precursors. In the longer run these tools will be used to identify moieties in both the extract and in young soots as these data will be useful in identifying the transition from the material in the vapor phase, particularly tars, to the solid. The techniques being used here were developed for examining the transition from coals to tars during devolatilization and are therefore ideally suited for this purpose, other than their requirement for larger sample sizes than can normally be acquired in well-defined laboratory flames. The requirement for large sample sizes is the reason that these preliminary experiments have been carried out with unextracted soot samples. Experimental procedures that will produce samples of sufficient size to permit solid state NMR studies of extracts and residues are presently underway.

Because of its noninvasive/nondestructive nature and sensitivity to subtle chemical structural features such as isomeric forms, nuclear magnetic resonance spectroscopy (NMR) has emerged as a major tool for characterizing complex structures. NMR experiments have been especially important for studying coal structure, reactivity, and pyrolysis products.<sup>21–30</sup> These data pro-

vided the critical information used to develop the chemical percolation devolatilization model (CPD)<sup>30</sup> which is now used to model combustion processes in industry and to model polymer thermal degradation at Sandia National Laboratories.<sup>31</sup> Solid state NMR spectroscopy techniques, while less sensitive than chromatography and mass spectroscopy methods, can be used to provide useful new information for bulk characterization of the chemical structural features of soot and soot precursors or their combination found in the aerosols produced during pyrolysis or partial combustion. Experimental techniques have been developed to produce suitable samples (based on quantity and formation temperature) for which NMR techniques can be employed to identify the average chemical structural features of aerosol particles in the early stages of formation and growth.

This paper presents data obtained by means of NMR techniques on aerosol samples made from an Illinois No. 6 coal and two model compounds, biphenyl and pyrene. Of particular interest in this study is the pyrolysis temperature at which transformation of aromatic hydrocarbons to PAH's (and eventually to soot) occurs for different simple aromatic starting materials. Particle agglomeration ultimately occurs in the soot evolution process. In the latter stages of particle growth the material becomes highly conductive, which limits the amount of NMR data that can be obtained during this stage in the structure evolution. Hence, the present work was designed to study the early to intermediate stages of soot production where changes in chemical structure can be observed. These changes can serve as a basis for developing/testing models of PAH evolution in the soot growth process.

## Experimental Section

**1. Coal Sample and Model Compounds.** An Illinois No. 6 coal and two aromatic model compounds were used to generate aerosol samples for subsequent solid-state <sup>13</sup>C NMR analysis. The elemental analysis of the coal and coal aerosol samples was provided by Galbraith Laboratories. The C, H, and N determinations were performed by combustion using a Leco CHN 1000 analyzer. Oxygen was determined by pyrolysis

(9) Graham, S. C. *Proc. R. Soc. London* **1981**, A377, 119–145.

(10) Mauss, F. Entwicklung eines kinetischen Modells der Russbildung mit schneller Polymerization. Ph.D. Thesis, RWTH, Aachen, 1998.

(11) Böhm, H.; Jander, H.; Tanke, D. *Twenty-Seventh Symposium (International) on Combustion*; The Combustion Institute: 1998; p 1605.

(12) Krestin, A. V. *Twenty-Seventh Symposium (International) on Combustion*; The Combustion Institute: 1998; p 1557.

(13) D'Anna, A.; Violi, A. *Twenty-Seventh Symposium (International) on Combustion*; The Combustion Institute: 1998; p 425.

(14) Wornat, M. J.; Sarofim, A. F.; Lafleur, A. L. *Twenty Fourth Symposium (International) on Combustion*; The Combustion Institute: 1992; p 955.

(15) Mukherjee, J.; Sarofim, A. F.; Longwell, J. P. *Combust. Flame* **1994**, 96, 191.

(16) Mulholland, J. A.; Mukherjee, J.; Sarofim, A. F. *Energy Fuels* **1997**, 11, 392.

(17) Homann, K. H.; Mochizuki, M.; Wagner, H. G. *Z. Phys. Chem.* **1963**, 37, 299.

(18) Bittner, J. D.; Howard, J. B. *Fourteenth Symposium (International) on Combustion*; The Combustion Institute: 1981; p 1105.

(19) Bhargava, A.; Westmoreland, P. R. *Combust. Flame* **1998**, 115, 456.

(20) Dobbins, R. A.; Fletcher, R. A.; Cheng, H.-C. *Combust. Flame* **1998**, 115, 285.

(21) Solum, M. S.; Pugmire, R. J.; Grant, D. M. *Energy Fuels* **1989**, 3, 187.

(22) Orendt, A. M.; Solum, M. S.; Sethi, N. K.; Pugmire, R. J.; Grant, D. M. In *Advances in Coal Spectroscopy*; Plenum Press: New York, 1992; Chapter 10, p 215.

(23) Fletcher, T. H.; Solum, M. S.; Grant, D. M.; Pugmire, R. J. *Energy Fuels* **1992**, 6, 643.

(24) Solomon, P. R.; Fletcher, T. H.; Pugmire, R. J. *Fuel* **1993**, 72, 587.

(25) Pugmire, R. J. Coal Structure from Solid State NMR In *Encyclopedia of NMR*; Grant, D. M., Harris, R. K., Eds.; John Wiley & Sons Ltd.: New York, 1996; p 1355.

(26) Watt, M.; Fletcher, T. H.; Bai, S.; Solum, M. S.; Pugmire, R. J. *Twenty-Sixth Symposium (International) on Combustion*; The Combustion Institute: 1996; p 3153.

(27) Kelemen, S. R.; Siskin, M.; Homan, H. S.; Pugmire, R. J.; Solum, M. S. Fuel, Lubricant and Additive Effects on Combustion Chamber Deposits. SAE No. 982715; 1998.

(28) Kelemen, S. R.; Siskin, M.; Most, W. J.; Kwiatek, P. J.; Pugmire, R. J.; Solum, M. S. Combustion Chamber Deposits from Base Fuel and Commercial IVD Detergent Packages. SAE No. 982716; 1998.

(29) Perry, S. T.; Hambly, E. M.; Fletcher, T. H.; Solum, M. S.; Pugmire, R. J. *Proceedings of the Combustion Institute*, 28; 2000; p 2313.

(30) Grant, D. M.; Pugmire, R. J.; Fletcher, T. H.; Kerstein, A. R. *Energy Fuels* **1989**, 3, 175. Fletcher, T. H.; Kerstein, A. R.; Pugmire, R. J.; Grant, D. M. *Energy Fuels* **1990**, 4, 54. Fletcher, T. H.; Kerstein, A. R.; Pugmire, R. J.; Grant, D. M. *Energy Fuels* **1992**, 6, 414.

(31) Hobbs, M. L.; Erickson, K. C.; Tze, Y. C. *Polym. Degradation Stab.* **2000**, 69, 47.

**Table 1. Elemental Analysis of Coal and Aerosol Samples<sup>a</sup>**

samples	C (%)	H (%)	N (%)	O (%)	H/C
Illinois No. 6 coal (daf) <sup>b</sup>	75.7	5.16	1.50	12.8	0.82
coal aerosol (1160 K)	78.2	5.02	1.75	11.3	0.76
coal aerosol (1280 K)	85.6	4.00	1.89	4.2	0.56
coal aerosol (1410 K)	89.4	3.19	1.36	2.7	0.43
coal aerosol (1530 K)	90.2	1.73	0.60	3.4	0.22
coal aerosol (1850 K)	90.1	1.18	0.56	3.1	0.16

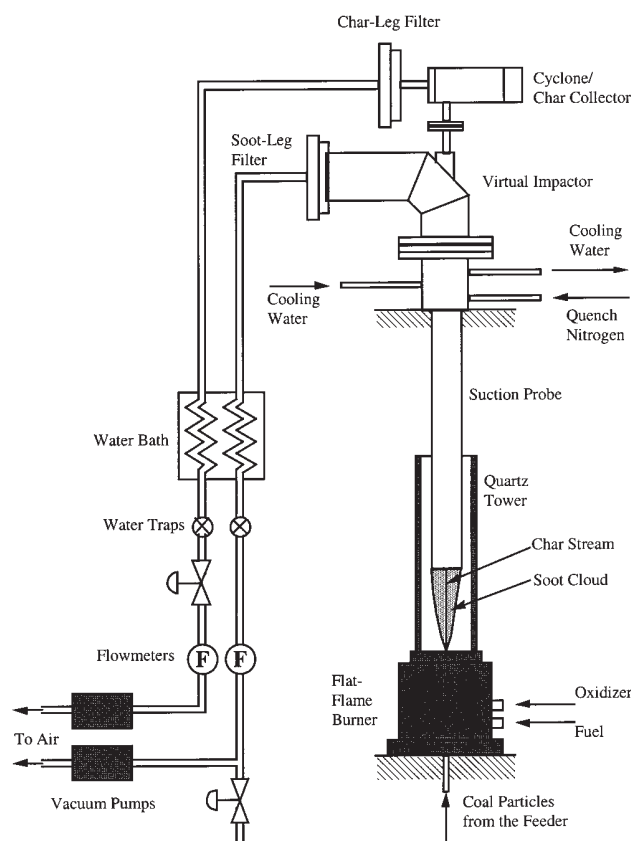
<sup>a</sup> The coal sample had a complete ultimate analysis but due to limitations in sample quantity only direct C, H, N, and O determinations were obtained on the aerosol samples. Since sulfur and ash were not determined, the percentages do not add to 100%.

<sup>b</sup> The coal sample also had 4.6% S (daf) and 0.24% Cl (daf) and 12.26 ash (AR).

using a modified Perkin-Elmer 240 elemental analyzer. The results of the aerosol sample analyses are presented in Table 1. Pyrene and biphenyl samples were obtained from the Aldrich Chemical Co. Elemental analysis of the model compound aerosol samples was not attempted due to contamination by silica gel used to entrain the samples (see below). The coal samples were dried in an oven for 2 h at 105 °C prior to the experiment in order to remove moisture. The coal samples and model compounds were ground and sieved to the diameter range of 45–75 μm. A 2:1 ratio of silica gel to model compound was used. The aerosol samples were analyzed for ash using the ASTM proximate procedure. The ash is obviously small SiO<sub>2</sub> particles from the silica gel. The biphenyl aerosols contained ca. 70% ash, while the pyrene aerosols contained only 10 to 25% ash. Tar/soot samples from the coal generally contained less than 1% ash.<sup>32</sup> The presence of the silica gel did not interfere with the NMR analysis, but did interfere with the elemental analysis due to the hydrophilic nature of silica. Catalytic effects are thought to be negligible.

**Flat Flame Burner.** The flat flame burner (FFB), which was designed originally for coal pyrolysis and combustion experiments, was used in this study to generate aerosol samples from both coal and model compounds. The schematic of the reactor is given in Figure 1; a detailed description can be found elsewhere.<sup>33,34</sup> A syringe-type particle feeder was used to provide a steady feed rate (~1 g/h) and to allow an accurate measurement of the total amount of sample fed in each experiment. This flow rate ensured single particle behavior in the reactor. The particles from the feeder were entrained in N<sub>2</sub> and injected about 1 mm above the burner surface through a metal centerline tube.

The temperature in the FFB can be adjusted by changing fuel type, the amount of dilution with N<sub>2</sub>, and the equivalence ratio. The typical heating rate for pulverized coal particles in this experiment has been calculated as approximately 10<sup>5</sup> K/s,<sup>33</sup> which is close to particle heating rates in industrial furnaces. The entire reactor can be raised and lowered relative to the level of the sampling probe to accommodate desired residence times. All the reaction products were collected by a water-cooled probe with nitrogen quench jets at the probe tip. Nitrogen was also transpired through a porous inner wall of the probe in order to minimize aerosol deposition on the probe walls. A virtual impactor at the end of the suction probe was used to separate the small and low-density aerosol particles from large, dense char particles (in the case of coal pyrolysis). The aerosol samples were collected on polycarbonate filters

**Figure 1.** Schematic of the flat flame burner (FFB).

with 1 μm pore diameters. Aerosol samples were carefully scraped from the filters to avoid the use of solvents.

**Reactor Temperature.** Temperature is a critical parameter in soot formation. Large PAH soot precursors start to form at about 1300 K in simple hydrocarbon flames. However, for a complicated compound like coal, the incipient temperature for soot precursor formation can be as low as 1100 K. The FFB was originally designed for high temperature, high heating-rate pyrolysis and combustion experiments. Methane was the design fuel and the temperature was controlled by manipulating the equivalence ratio. However, the lowest operating temperature of fuel-rich methane flames was found to be about 1600 K due to the narrow flammability limits of CH<sub>4</sub> (5% to 15%, by volume in air). This observation is consistent with the report by Glassman et al.<sup>35</sup> that the temperature at which soot luminescence appears is the same for all fuels (approximately 1600 K). Since the chemical properties of incipient soot and soot precursors are of special interest in this study, temperatures as low as 1100 K are desired in the FFB. This was achieved by using carbon monoxide (CO) for the fuel in the FFB. CO has much broader flammability limits (12.5% to 75%, by volume in air) than most of common hydrocarbon fuels. Therefore, the temperature of a stable CO flame can be easily lowered to approximately 1100 K even at very fuel rich conditions. In practice, a small amount of hydrogen was also added to the fuel stream to enhance the combustion, since the CO–OH reaction is essential for rapid combustion. The equivalence ratio for a CO flame in the FFB was easily adjusted to vary the temperature between 1100 and 2000 K to facilitate the pyrolysis experiments. The total gas flow rate ranged from 19 to 26 slpm (air/N<sub>2</sub>/CO/H<sub>2</sub>), with equivalence ratios ranging from 1.45 at 1160 K to 1.0 at 1860 K. A flow rate of 0.04 slpm of N<sub>2</sub> was used to feed the particles into the

(32) Zhang, Z. Nitrogen Evolution and Soot Formation during Secondary Coal Pyrolysis. PhD Dissertation, Chemical Engineering Department, Brigham Young University, Provo, UT (April 2001).

(33) Ma, J.; Fletcher, T. H.; Webb, B. W. *Twenty-Sixth Symposium (International) on Combustion*; The Combustion Institute: 1996; p 3161.

(34) Ma, J. Soot Formation During Coal Pyrolysis. Ph.D. Dissertation, Chemical Engineering Department, Brigham Young University, Provo, UT (August, 1996).

(35) Glassman, I.; Nishida, O.; Sidebotham, G. Critical Temperatures of Soot Formation. In *Soot Formation in Combustion*; Bockhorn, H. Ed.; Springer-Verlag: New York, 1994; 316.

reactor. Exact gas flow rates for each condition are given by Zhang.<sup>32</sup> No soot was observed from these CO flames on the sample filters or by visible radiant emissions. Gas temperature profiles in each condition were measured using a bare thermocouple and correcting for radiation losses. Aerosol temperatures were assumed to be the same as the gas temperature. Temperature profiles of coal particles have been calculated for similar systems;<sup>36,37</sup> temperature profiles of the silica gel particles and model compound particles can be calculated in a similar manner if quantitative transformation rates are desired.

Aerosol samples were obtained at the 1 in. sampling height (50 ms) at the 1160 K condition and at the 3 in. height (70 to 80 ms) at all other temperatures. The color of the aerosol samples changed from light brown to black as the temperature increased for both coal and model compounds. The sample color serves as a rough visual metric for the extent of transformation from incipient soot formation to large soot particles.

**Sample Preparation for Model Compounds.** The model compounds, when ground to 45–75  $\mu\text{m}$ , were almost impossible to inject directly into the reactor because the particles adhered to the wall of the funnel and to the polyethylene transport tubing connecting the funnel and the reactor. Coal particles can be transported smoothly into the reactor because of the mineral matter in the coal. The mineral matter helps to maintain the skeleton of the coal particles and perhaps helps to reduce the surface tension or electrostatic forces between the particles and the wall. Pyrene and biphenyl particles become very “sticky” due to electrostatic forces when ground to small sizes. In this study, an inorganic material was mixed with the model compounds and then ground to fine powders ranging from 45 to 75  $\mu\text{m}$ ; this produced a mixture more like coal in order to use the current particle feeding system. Several inorganic compounds were tested, and silica gel was found to work well. Silica gel is not pyrolyzed or vaporized under the desired temperature conditions (1160–1470 K). The silica gel shows no color when injected into the hot flame, so there is no interference with the luminescent yellow cloud produced by soot particles. The luminosity caused by radiation from soot particles is the easiest way to identify the formation of soot in a combustion system. The model compounds, when mixed with silica gel, were easily transported into the reactor through the feed line. In addition, since silica gel has a much higher density than soot particles, it can be partially separated by the virtual impactor and collected by the cyclone used for collection of char in a coal experiment.

**2. NMR Data.** The standard one-dimensional analysis procedure (as described in the Appendix) was carried out on a Chemagnetics CMX-100 NMR spectrometer operating at a carbon frequency of 25.152 MHz and a proton frequency of 100.02 MHz. The spectrometer utilizes a 7.5 mm PENCIL rotor probe with a ceramic housing to remove carbon background. All CPMAS experiments were run with 62.5 kHz of decoupling power, corresponding to a proton 90° pulse of 4  $\mu\text{s}$  (for diamagnetic samples), a 1 s pulse delay, and a spinning speed locked to 4100 Hz. Four types of experiments were employed.

(1) A standard <sup>13</sup>C CPMAS experiment with a 2 ms contact time was taken for all samples except the 1530 K Illinois No. 6 aerosol where a longer contact time (10 ms) was necessary (due to the lower H/C content of this sample, see Table 1). The 1850 K Illinois No. 6 sample had such a low H/C ratio (see Table 1) that a single pulse, SP, experiment was used. A 2 ms contact time is the minimum contact time (4 to 5  $T_{\text{CHL}}$ ) necessary for polarization of nonprotonated carbons as can be seen by the  $T_{\text{CHL}}$  data in Table 2, which is typical for aromatic compounds. The one exception was the Illinois No. 6 aerosol produced at 1530 K where the  $T_{\text{CHL}}$  value for this sample increased to 858  $\mu\text{s}$ . Since the  $T_{1\rho}^{\text{H}}$  value also dramatically

**Table 2. Results from Variable Contact Time Experiments on the Coal and Aerosol Samples<sup>a</sup>**

sample	$T_{\text{CHL}}$ ( $\mu\text{s}$ )	$T_{1\rho}^{\text{H}}$ (ms)
Illinois No. 6 coal	415	4.0
Illinois No. 6 aerosol 1180 K	410	7.3
Illinois No. 6 aerosol 1280 K	266	4.2
Illinois No. 6 aerosol 1410 K	306	12.7
Illinois No. 6 aerosol 1530 K	858	75
biphenyl aerosol 1365 K	342	7.2
biphenyl aerosol 1410 K	334	7.8
biphenyl aerosol 1470 K	426	12.8
pyrene aerosol 1410 K	255	5.2
pyrene aerosol 1460 K	230	16.2

<sup>a</sup> An additional Gaussian time constant was used to account for the first stage of two stage crosspolarization of protonated carbons.<sup>22</sup> This time constant was 18  $\mu\text{s}$  for all samples. The error in  $T_{\text{CHL}}$  is on the order of 30% and the error in  $T_{1\rho}^{\text{H}}$  is on the order of 10%.

increased to 75 ms (see Table 2) this longer contact time of 10 ms was possible without the drastic reduction in the signal-to-noise ratio that would usually occur with a contact time this long in typical amorphous carbonaceous samples. The temperature designation of the sample refers to the nominal temperature of the flame or reactor in which the coal or model compounds are injected. The CPMAS NMR spectra of the Illinois No. 6 coal and all other coal aerosols were collected with 10 000 scans under the experimental conditions noted. The aerosol samples obtained from the model compounds required 70 000–165 000 scans due to the varying amount of silica gel (which diluted the product) used to entrain the solid samples. Data analyses for all of the model compound derived samples were carried out on these silica gel diluted products. Since subregion integrals are performed on these spectra more scans are taken on these spectra than on those described below where whole regions (aromatic or aliphatic) are integrated. The errors in these integrations are estimated at 1–2%.

(2) A variable contact time experiment was run with 21 different contact times ranging from 5  $\mu\text{s}$  to 25 ms. The results from this experiment were used to determine the carbon aromaticity independent of contact time. For both variable contact time and dipolar dephasing (described below) experiments the data were collected in an interleaved fashion where about 100 scans were collected for each value of the incremented variable. The whole cycle was repeated between 30 and 61 times for a total of 3000–6100 total scans for each value of the incremented variable.

(3) A dipolar dephasing experiment was run using a 2 ms (or 10 ms for the 1530 K coal sample) contact time, chosen after examination of the individual sample variable contact time data, and using pulse sequence B from ref 38. This experiment was run with 22 different dephasing times from 2  $\mu\text{s}$  to 180  $\mu\text{s}$  prior to the appearance of the first rotational echo which comes at 244  $\mu\text{s}$ . The proton content of one sample, the Illinois No. 6 aerosol made at 1850 K, was so depleted that a successful cross-polarization experiment was not possible. Hence, no variable contact time or dipolar dephasing experiments were performed on this sample.

However, a single pulse experiment (4) was performed on this 1850 K sample with a pulse delay of 10 s and accumulation of 14 976 spectral scans.  $T_1^{\text{C}}$  was not measured for this sample. The appearance of extensive line broadening prevented calculation of structural parameters, and hence, no analysis was attempted on this sample.

All Q value measurements were performed by placing either an empty 7.5 mm rotor or the same rotor containing the sample into a five-turn coil connected to a Booton Radio Corporation type 160-A Q-meter.

(36) Fletcher, T. H. *Combust. Sci. Tech.* **1988**, *63*, 89.

(37) Fletcher, T. H. *Combust. Flame* **1989**, *78*, 223.

(38) Newman, R. H. *J. Magn. Reson.* **1992**, *96*, 370.

**Table 3. Differences in Sample *Q* Values at 25 MHz**

sample	$Q_{\text{empty probe}} - Q_{\text{sample}}$
Illinois No. 6 coal	0
Illinois No. 6 aerosol, 1160 K	0
Illinois No. 6 aerosol, 1280 K	0
Illinois No. 6 aerosol, 1410 K	0
Illinois No. 6 aerosol, 1530 K	7
Illinois No. 6 aerosol, 1850 K	41
biphenyl	0
biphenyl aerosol, 1365 K	0
biphenyl aerosol, 1410 K	2
biphenyl aerosol, 1470 K	5
pyrene	0
pyrene aerosol, 1410 K	2
pyrene aerosol, 1460 K	5

## Results and Discussion

**Sample Conductivity.** It is well-known in the NMR community that highly conductive samples present special problems relating to probe tuning and associated degradation of sensitivity. In addition, highly conductive materials limit penetration of the NMR radio frequency into such samples, and this "skin depth" problem may limit the amount of data that can be obtained in these samples. A simple way to screen materials to identify potential conductivity problems is by determining the *Q* value of the sample. This is done by comparing the measured *Q* value of an empty NMR coil with that of the same coil containing the sample of interest. The differences in the *Q* values of the samples studied were measured at 25 MHz and the results are given in Table 3. In the case of the coal and coal-derived samples, changes in the *Q* values do not appear until a temperature of 1530 K is reached. The effect is quite pronounced in the sample obtained at 1850 K. Small increases in the *Q* values (2 units compared to the parent molecules) are observed in the 1410 K biphenyl and pyrene aerosol samples, while changes of 5 units are noted in the samples collected at 1460 and 1470 K, respectively. The NMR spectra of the samples in which changes in the *Q* values are observed also exhibit a component with Lorentzian line shape that underlies the aromatic band.

**Illinois No. 6 Soots.** The <sup>13</sup>C NMR spectra of the original coal and each Illinois No. 6 aerosol sample are given in Figure 2. The spectrum for the coal and the four lowest temperature aerosol samples was obtained by means of the CP experiment. The contact time was 2 ms for the lower temperature samples and the coal and, due to proton depletion, a 10 ms value was necessary for adequate cross-polarization of the 1530 K sample. The sample at 1850 K had so few protons that the CP experiment failed and a SP experiment was used to obtain the spectrum. The structural and lattice parameters for these samples are given in Table 4.

An aromaticity value of 0.72 was determined for the original coal while the average aromatic cluster size is 15 (see definitions in the Appendix). Clear shoulders can be seen on the aromatic band at about 140 ppm for substituted aromatic carbons and at 154 ppm for oxygenated aromatic carbons. The fraction of carbonyl/carboxyl carbon in this sample is 0.05. In the aliphatic region the methylene/methine and methyl group fractions are 0.19 and 0.09, respectively.

The aerosol sample at 1160 K has a higher aromaticity, 0.85, than that of the coal while the cluster size

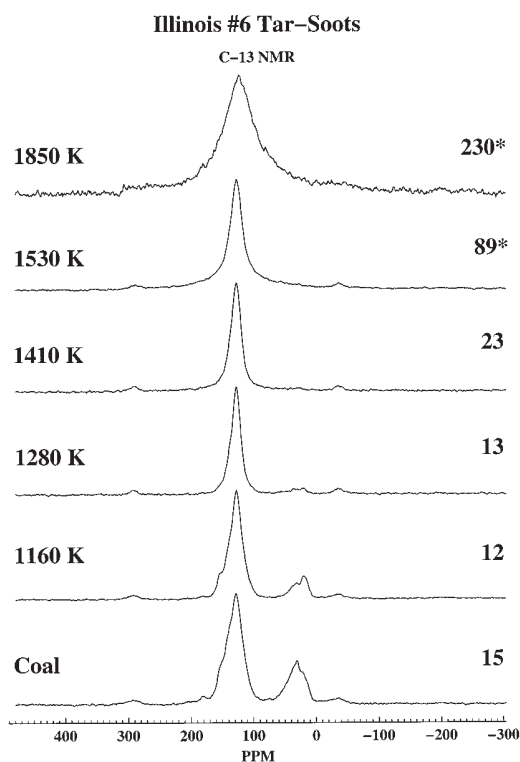


**Figure 2.** <sup>13</sup>C CPMAS (SP experiment for 1850 K) spectra of Illinois No. 6 coal and aerosol samples. Flat flame burner temperatures are on the left while average aromatic cluster size is given on the right side of each spectrum. The asterisks indicate maximum cluster size estimates.

decreases to a value of 12. In the parent coal all sp<sup>2</sup> signals (not counting carboxyls/carbonyls) are expected to arise from aromatic carbons. However, in the low temperature aerosols some ethylenic and acetylenic carbons may be present and the spectral response from these types of structures would report in the same band as the aromatic carbons. The smaller cluster size in the 1160 K aerosol (12 vs 15 in the parent coal) suggests that smaller PAHs are liberated from the lattice, enter the gas phase and are collected as aerosol while, on average, slightly larger clusters (or more extensively cross-linked clusters) are retained in the solid coal lattice (this phenomenon has been documented in matched tar/char sets<sup>29</sup>). The sample collected at 1280 K has a slightly higher cluster size (13), but this value is still lower than that observed in the original coal. The aromaticity parameter of this sample is 0.92. As the temperature is increased from room temperature to 1280 K the NMR data indicates that the ratio of methyl groups to methylene/methine groups increases. On the other hand, the carbonyl and carboxyl groups display a decreasing trend and essentially have disappeared at temperatures above 1280 K. Phenolic groups also decrease as can be seen by the decrease in the shoulder at 154 ppm. The fraction of the carbons associated with phenolic/ether structures  $f_a^P$  (see Table 4) is the same as that for the 1160 K sample as for the coal even though the phenolic shoulder clearly decreases. This apparent anomaly arises because the aliphatic content has also decreased and this parameter is based on 100 total carbons. The relative amount of phenolic aromatic

Table 4. Structural and Lattice Parameters for Illinois No. 6 Aerosols

compound	structural parameters													
	$f_a$	$f_a^C$	$f_a^O$	$f_a^{OO}$	$f_{a'}$	$f_a^H$	$f_a^N$	$f_a^P$	$f_a^S$	$f_a^B$	$f_{al}$	$f_{al}^H$	$f_{al}^*$	$f_{al}^O$
coal	0.72	0.05	0.02	0.03	0.67	0.21	0.46	0.08	0.18	0.20	0.28	0.19	0.09	0.05
1160 K	0.85	0.04	0.02	0.02	0.81	0.33	0.48	0.08	0.19	0.21	0.15	0.09	0.06	0.02
1280 K	0.92	0.02	0.005	0.015	0.90	0.42	0.48	0.04	0.19	0.25	0.08	0.05	0.03	0.02
1410 K	0.97				0.97	0.33	0.64	0.00	0.19	0.45	0.03	0.03	0.00	
1530 K	1.00				1.00	0.26	0.74			0.74	0.00	0.00	0.00	

compound	lattice parameters								
	$\chi_b$	$C$	$\sigma + 1$	$P_0$	B.L.	S.C.	MW	$M_b$	
coal	0.299	15	5.8	0.65	3.8	2.0	355	24	
1160 K	0.259	12	4.0	0.78	3.1	0.9			
1280 K	0.278	13	3.3	0.87	2.9	0.4			
1410 K	0.464	23	4.5	1.00	4.5	0.0			
1530 K	0.74	89		1.00					

carbon  $f_a^P/f_{a'}$ , does decrease as does  $f_a^S/f_{a'}$  even though the amount of substituted aromatic carbon  $f_a^S$  remains constant.

The sample obtained at 1410 K indicates that between 1280 and 1410 K major structural changes occur. If one carefully examines the 1410 K spectrum a very broad component can be detected under the normal aromatic band. The structural parameters obtained for this sample were determined by employing a deconvolution technique to the line shape rather than the usual spectrum integral ranges (see the Appendix). The average aromatic cluster size has increased to over 20 carbons at 1410 K. The cluster size parameter implies that secondary reactions have occurred in the gas phase following liberation of a smaller aromatic cluster (e.g., ca. 12) from the coal lattice. If the usual integral ranges were used in the analysis of this spectrum then three parameters,  $f_a^C$ ,  $f_a^P$ , and  $f_{al}^O$ , the values of which have decreased from those found in the coal, start to increase again for this sample. This increase appears to be due to the presence of a broad signal of Lorentzian character that underlies the normal aromatic resonance signal and may not be due to formation of oxygen functional groups. A direct elemental analysis for oxygen reported only two oxygen atoms per 100 carbons and, hence, the intensity observed cannot be due entirely to oxygen functional groups. The two highest temperature aerosols, obtained at 1530 and 1850 K, contained only 2–3 oxygen atoms per 100 carbons. This broad component, which dominates the line shape for the two highest temperature aerosols, indicates that a structural change in the samples is associated with the transition from early light tar materials to much larger aromatic structures. Only a small amount of the larger soot particles is probably present in this 1410 K sample since the probe  $Q$  value has not changed from the empty coil value shown in Table 3.

The line width of the 1530 and 1850 K samples exhibit additional broadening associated with increasing temperature. The specific source of this broadening mechanism is not known at this time. The two highest temperature samples appear to be composed entirely of aromatic structures. The parameters used to obtain the NMR spectra of these two samples suggest that a substantial decrease in H/C has occurred (which is substantiated by a decrease of 27% in H/C, see Table 1) between 1530 and 1850 K. Hence, the coal soot samples provide a means for determining the temperature range

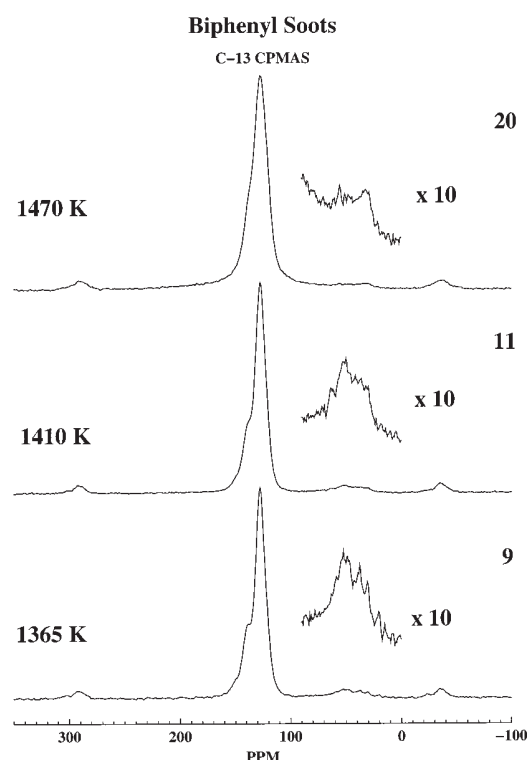


Figure 3.  $^{13}\text{C}$  CPMAS spectra of biphenyl aerosol samples produced at temperatures indicated. The  $\times 10$  inserts focus on the presence of aliphatic carbons present in each sample. The 1470 K sample illustrates the Lorentzian component of the aromatic band which, at this temperature, begins to obscure the aliphatic structure in the sample.

that is useful for study of incipient soot formation and growth prior to the formation of large graphite-like structures.

**Biphenyl Soots.** Three aerosol samples were prepared by pyrolysis of entrained biphenyl in the flat flame burner at temperatures of 1365, 1410, and 1470 K. Biphenyl is a simple biaryl aromatic system (average aromatic cluster is defined as 6 carbons) that does not contain any bridgehead carbon. The quaternary carbons are substituted aromatic carbons that span a zero mass bridge between two aromatic clusters. CPMAS spectra for each of the biphenyl aerosol samples, taken with a 2 ms contact time, are shown in Figure 3 and the structural and lattice parameters are given in Table 5. Each of the spectra exhibit a large aromatic signal centered at about 127 ppm with a very prominent

**Table 5. Structural and Lattice Parameters for Model Compound Aerosols**

structural parameters														
compound	$f_a$	$f_a^C$	$f_a^O$	$f_a^{OO}$	$f_a'$	$f_a^H$	$f_a^N$	$f_a^P$	$f_a^S$	$f_a^B$	$f_{al}$	$f_{al}^H$	$f_{al}^*$	$f_{al}^O$
biphenyl	1.00	0.00	0.00	0.00	1.00	0.83	0.17	0.00	0.17	0.00	0.00	0.00	0.00	0.00
1365 K	0.91	0.00	0.00	0.00	0.91	0.54	0.37	0.03	0.20	0.14	0.09	0.08	0.01	
1410 K	0.93	0.00	0.00	0.00	0.93	0.50	0.43	0.02	0.19	0.22	0.07	0.07	0.00	
1470 K	0.98				0.98	0.36	0.62	0.04	0.19	0.39	0.02	0.02	0.00	
pyrene	1.00	0.00	0.00	0.00	1.00	0.625	0.375	0.00	0.00	0.375	0.00	0.00	0.00	0.00
1410 K	0.98	0.02	0.00	0.02	0.96	0.47	0.49	0.02	0.12	0.35	0.02	0.02	0.00	
1460 K <sup>a</sup>	0.99				0.99	0.36	0.63		0.05	0.58	0.01	0.01	0.00	
1460 K <sup>b</sup>	0.99				0.99	0.36	0.63	0.03	0.13	0.47	0.01	0.01	0.00	

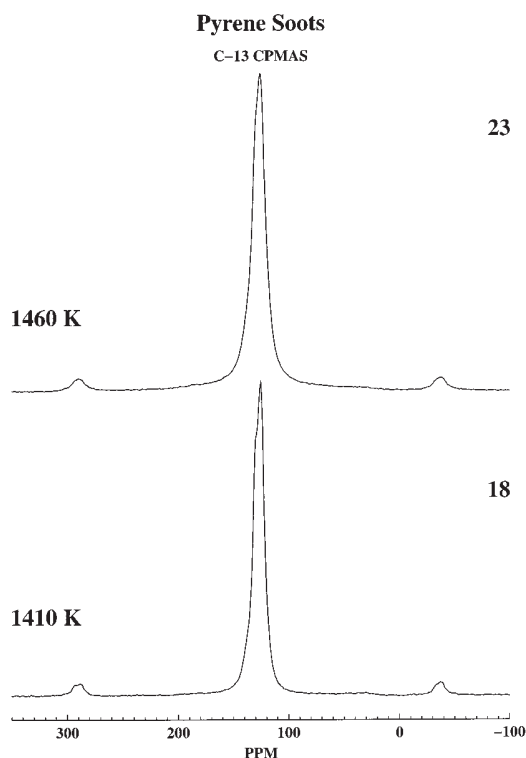
  

lattice parameters									
compound	$\chi_b$	C	$\sigma + 1$	$P_0$	B.L.	S.C.	MW	$M_\delta$	
biphenyl	0.000	6	1.0	1.00	1.0	0.0	77	0	
1365 K	0.154	9	2.3	0.96	2.2	0.1			
1410 K	0.237	11	2.5	1.00	2.5	0.0			
1470 K	0.398	20	4.7	1.00	4.7	0.0			
pyrene	0.375	16 (18.6) <sup>c</sup>	0.0	0.00	0.0	0.0	202	0	
1410 K	0.365	18	2.6	1.00	2.6	0.0			
1460 K <sup>a</sup>	0.586	35	1.8	1.00	1.8	0.0			
1460 K <sup>b</sup>	0.475	23	3.7	1.00	3.7	0.0			

<sup>a</sup> Determined by deconvolution of the CPMAS spectrum. <sup>b</sup> Determined by the shift ranges given in the Appendix. <sup>c</sup> The actual cluster size is 16. If one uses our cluster size model that is a combination of the circular and linear catenation models then, based on the mole fraction of bridgehead carbon, the value is estimated at 18.6. Of all the aromatic compounds used to construct the cluster size model, pyrene represented the largest deviation from the analytical function used to describe average cluster size in PAHs (see ref 21).

shoulder at about 140 ppm attributed to the presence of substituted (alkyl and/or aryl groups) aromatic carbons. A less prominent component at approximately 150 ppm indicates the presence of small contributions from phenolic structures  $f_a^P$  or the substituted carbons of biphenylene which has an isotropic chemical shift of 151–152 ppm.<sup>39</sup> The aliphatic region of each spectrum exhibits a rather broad but distinct signal accounting for 9%, 7%, and 2% of the total carbon observed at temperatures of 1365, 1410, and 1470 K, respectively. The presence of aliphatic structures in all three samples is clear (note  $\times 10$  inserts) and indicates that ring opening coupled with hydrogen transfer reactions have occurred. The aromatic line-shape of the 1470 K sample exhibits contribution from Lorentzian wings, similar to that observed in the 1530 and 1850 K coal aerosol samples, suggesting that graphene-like (large PAH) structures are beginning to form in this temperature regime. The Lorentzian character of the aromatic line shape at this temperature obscures the carboxyl/carbonyl regions of this spectrum.

The dipolar dephasing experiments indicate that bridgehead carbons have formed at even the lowest temperature (1365 K) and that aromatic ring growth has occurred to the extent that the average aromatic cluster has increased by 50%, e.g., nine carbons. The cross-linking parameter (B.L.) has increased from 1.0 in biphenyl to an average of 2.2 in this sample (see Figure 5). In the 1410 K sample the cluster size has increased further to about 11 carbons per cluster, with the cross-linking slightly increasing to 2.5 per cluster. The sample at 1470 K shows a large increase in the cluster size to 20 carbons, with an additional large increase in the cross-linking parameter (i.e., 4.7 per cluster). The dipolar dephasing experiments allows one to partition the total fraction of nonprotonated aromatic carbon into phenolic carbons, substituted carbons and



**Figure 4.** <sup>13</sup>C CPMAS spectra of pyrene aerosol samples collected at 1410 and 1470 K. Spinning sidebands are noted ca. 300 and –40 ppm. Note the very small amount of aliphatic carbon (ca. 1–2%).

bridgehead carbons. When the sample shows large Lorentzian wings, selected chemical shift integration ranges used to separate phenolic from substituted carbons become less precise. If the dipolar dephasing fraction of nonprotonated aromatic carbon  $M_L$  (see the Appendix) is assumed to represent only bridgehead carbon then one can obtain only an upper limit for the aromatic cluster size. Cartoons illustrating the critical lattice parameters (cluster size and cross-links per

(39) Barich, D. H.; Orendt, A. M.; Pugmire, R. J.; Grant, D. M. *J. Phys. Chem.* **2000**, *104*, 8290.

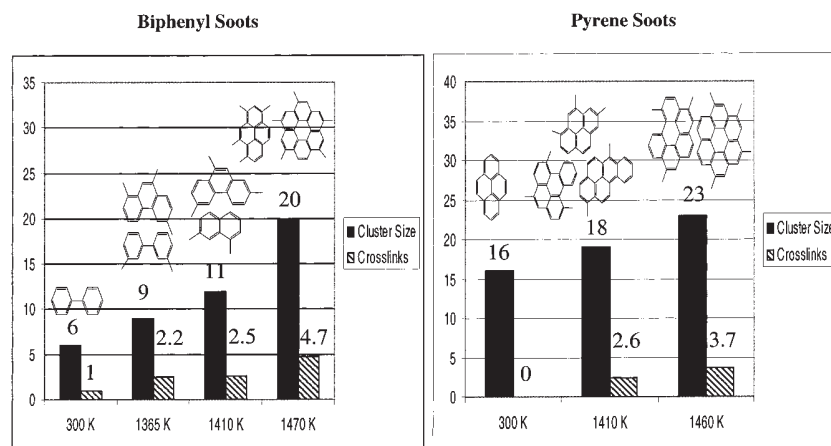


**Figure 5.** Average structural information (bar graphs) derived from  $^{13}\text{C}$  NMR data obtained on aerosol samples of biphenyl and pyrene. Average cluster size (aromatic carbons per aromatic cluster) and number of cross-links per cluster are given for the model compound as well as for each aerosol sample studied. Molecular structures are suggestive of the types of materials that are present in the various aerosol samples.

cluster) together with representative structures are given in Figure 5.

**Pyrene Soots.** Two aerosol samples prepared at 1410 and 1460 K from pyrene were also studied. The original pyrene molecule contains 16 total aromatic carbons consisting of 6 bridgehead and 10 protonated carbons. The original molecule has no substituted carbon atoms and no cross-links. The 1410 K sample contains only about 2% aliphatic material, much less than the 7% observed in the corresponding biphenyl sample. This observation indicates that the extent of ring opening reactions in pyrene is substantially less than that observed in the corresponding biphenyl derived sample. However, the cross-linking parameter at this temperature, as determined by the appearance of substituted carbons, indicates that the number of cross-links per cluster is similar to that observed in the corresponding biphenyl sample (e.g., 2.5) while the cluster size is not significantly larger than the parent compound (e.g., 18 vs 16, see footnote "c" to Table 5). The cross-links probably arise from biaryl linkages since the amount of substituted carbons per cluster exceeds the amount of aliphatic material present. It appears that observable amounts of dimers and trimers have been formed without significant growth in the aromatic cluster size. The formation of aryl polymers is consistent with data observed by Sarofim and co-workers in pyrolysis studies of anthracene<sup>14</sup> and pyrene.<sup>15,16</sup> High-resolution mass spectroscopy data confirm the presence of monomers as well as dimers and trimers of pyrene at both 1410 and 1460 K, but these materials are present in smaller amounts at the higher temperature.<sup>40</sup>

The pyrene aerosol at 1460 K contains only about 1% aliphatic material, with Lorentzian wings quite evident in the aromatic band. At this temperature it appears that a major structural change has occurred. The Lorentzian wings in the spectrum are indicative that graphene-like structures have begun to form and that the spectral response from such structures are overlaid on the signals from a wide variety of PAH's. Hence, the Lorentzian wings obscure resonances from carbonyl/carboxyl, phenolic and substituted groups that might

be present in the aerosol. This condition compromises the standard data analysis techniques described in the Appendix and leads to some uncertainty in partitioning magnetization arising from either substituted carbons in PAHs or contributions from nonprotonated carbons in graphene-like structures.

The spectrum of this sample can be analyzed by three alternative methods. The first alternative ignores the contributions of the Lorentzian wings and assumes that magnetization appearing in the normal chemical shift/integration range can be attributed to substituted ( $f_a^S$  and  $f_a^P$ ) carbons. This alternative yields an average cluster size of 23 aromatic carbons with 3.7 attachments per cluster. A second method involves a standard deconvolution of the aromatic band observed in the CPMAS spectrum that yields a lower fraction of substituted carbons per cluster (1.8) but a larger average aromatic cluster size (35 carbons per cluster). The third alternative utilizes the data obtained from the dipolar dephasing experiment and assumes that all nonprotonated carbons are bridgehead carbons. This assumption would place an upper limit of the cluster size at 46 carbons with no detectable cross-links. On the basis of the laser desorption mass spectroscopy data obtained on this sample,<sup>40</sup> an average cluster size of 46 is not likely since molecular ions of that size were not observed. On the other hand, the weighted average of the molecular ions observed is less than 30 carbons.

It is interesting to note that the Lorentzian contributions to the NMR spectral line shape occur at approximately the same temperature in the coal aerosols, the biphenyl aerosols and the pyrene aerosols. This observation suggests that the appearance of large aromatic structures occur at approximately 1500 K and this observation is consistent with data reported by Glassman<sup>35</sup> regarding the minimum temperature for formation of soot particles from hydrocarbon fuels.

## Conclusions

Aerosol samples produced from an Illinois No. 6 coal (five samples) and two model compounds, biphenyl (three samples) and pyrene (two samples), have been studied by  $^{13}\text{C}$  NMR methods. The coal soot data served

(40) Winans, R. E.; Pugmire, R. J. 2000. Unpublished data.

as a guide to selection of the temperature range that would be most fruitful for investigation of the evolution of soot samples obtained from model compounds. The evolution of the different materials in the gas phase followed different paths. The coal derived soots exhibited loss of aliphatic and oxygen functional groups prior to significant growth in average aromatic cluster size. Between 1410 and 1530 K, line broadening occurs in the aromatic band, which appears to have a Lorentzian component that is observable at the lower temperature and is quite pronounced at the higher temperature. The data on the 1530 K sample indicate that the average aromatic cluster size may be as large as 80–90 carbons/cluster. The 1850 K sample is dominated by a line broadening mechanism, and little useful information can be obtained except to note that the average cluster size is now very large (as large as 230 carbons), as evident from a H/C value of 0.16. The number of side chains as well as bridges and loops, which is a measure of potential cross-linking sites, declines with temperature as functional groups are eliminated during the early stages of soot formation. However, at 1410 K no aliphatic side chains are evident but the number of bridges and loops increases significantly (by 50% to 4.5 per cluster), suggesting that ring polymerization reactions may have taken place. Because of the Lorentzian line shape that now becomes significant at 1530 K, it is no longer possible to estimate the value of this parameter.

The data obtained for the biphenyl samples exhibit a different path for pyrolysis and molecular weight growth. First, ring opening reactions have occurred in the samples, which is clearly evident by the amount of aliphatic carbon present at all three temperatures. However, the fraction of aliphatic carbon (primarily CH and CH<sub>2</sub>) decreases with temperature (e.g., 0.09, 0.07, and 0.02), indicating that major structural rearrangements are occurring following the initial ring opening and hydrogen transfer phase. The amount of cluster cross-linking, which is 1 in unreacted biphenyl, doubles to 2.2 and 2.5 at 1365 and 1410 K, and then doubles again to 4.7 at 1470 K. The cluster size, which starts at 6 in the parent molecule, grows to 9, 11, and 20 aromatic carbons, respectively. Hence, the cluster size not only grows significantly but the cross-linking structure also increases from a value of 1 to nearly 5 over the relevant temperature range. This suggests that molecular weight growth in biphenyl soots consists not only of cluster size growth but also cluster cross-linking which could result in the formation of large cross-linked structures. This transformation to relatively large tar/soot structures is manifest in the NMR spectra not only as large Lorentzian wings on the aromatic signal, but is also accompanied by a loss of functional groups, a loss of aliphatic material, an increase in bridging structures, and an increase in the average aromatic cluster size.

The evolution of pyrene aerosols follows still another path. First, little evidence is noted for ring opening reactions as only ca. 1% of the carbon appears as sp<sup>3</sup> hybridized species, indicating that very little ring opening occurs, or at least that stable alicyclic molecular species are formed following ring opening. Second, ring growth of only approximately 10% has occurred at 1410 K compared to nearly 100% in the case of the corre-

sponding biphenyl aerosols. However, data on this 1410 K aerosol sample indicate that the relatively small cluster size has been augmented by an average of 2.6 cross-link sites per cluster. The Lorentzian character of the aromatic band, which becomes apparent at 1460 K, makes it difficult to estimate the cluster size and number of cross-links per cluster. Data analysis based on deconvolution of the broadened aromatic band suggests ring growth to an average size of 35 carbons per cluster with a decrease in cross-link sites to 1.8 per cluster. This analysis would support the cyclodehydrogenation pathways proposed by Mukherjee et al.<sup>15,16</sup> as the means of molecular weight growth. If, however, the data are analyzed by employing the normal integration ranges described in the Appendix the results are quite different. This analysis procedure estimates a much smaller average cluster size (23) and twice the number of cross-link sites (3.7). This analysis would suggest that the cyclodehydrogenation reactions proposed by Mulholland et al.<sup>16</sup> are not yet the dominant mechanisms of ring growth at this temperature. However, the large number of cross-link sites per cluster suggests that a significant amount of cluster polymerization has occurred. Hence, the data are inconclusive regarding the mechanism for ring growth in the pyrene tar/soots between 1410 and 1460 K.

**Acknowledgment.** Work at the University of Utah was supported by the Department of Energy as part of the Advanced Strategic Computing Program (ASCI) through contract number B341493 from Lawrence Livermore National Laboratory and the DOE Fossil Energy/National Petroleum Technology Office (FE/NPTO) contract No. DE-AC 26-99BC, and by the National Science Foundation under NSF CRAEMS grant CHE 0089133. Q value measurements were supplied by Y. J. Jiang. Work carried out at Brigham Young University was supported by the DOE University Coal Research Program through contract number DE-P522-97PC97200.

## Appendix

The carbon skeletal structure of carbonaceous materials (soots in this case) is determined by a combination of three NMR experiments. The first is a variable contact time experiment that determines the carbon aromaticity independent of contact time. The second is a dipolar dephasing experiment that differentiates protonated from nonprotonated aromatic carbons. This dipolar dephasing experiment could also be used in the aliphatic region to separate nonprotonated aliphatic carbons and methyl groups from methylene and methine groups. The third NMR experiment is a standard CPMAS spectrum taken with a contact time long enough (2–10 ms is usually sufficient) to fully polarize all types of carbons in the sample. From the cross-polarization spectra, subintegral ranges are chosen that pertain to different types of functional groups. The exact chemical shift ranges used for the subintegrals may need to vary depending on the exact type of materials being analyzed. The integral ranges given below are for standard hydrocarbons having only one or less oxygen attachment per aromatic ring. These shift ranges were chosen for bituminous coals and are good for tars and soots but would need to be modified for very low rank

materials such as lignins which have two or three oxygen substitutions on a single aromatic ring.<sup>41</sup> In addition, these standard integral ranges are not satisfactory for the analysis of samples that display excessive line broadening even though an NMR spectrum can still be obtained. The terms described below define the meaning of the symbols in the structural and lattice parameter tables.

All of the structural parameters are defined on a fractional basis and when multiplied by 100 are transformed to a 100 carbon atom basis. A variable contact time experiment is used to determine the aromaticity  $f_a$  and the aliphaticity  $f_{al}$ , which, by this experiment are essentially independent of contact time. These parameters are determined by fitting the magnetization of each of the two main spectral regions, aromatic and aliphatic, separately as a function of the contact time to the appropriate standard equation as described in ref 22. The total magnetization of each region is given by

$$f_a = \frac{M_{ar}}{M_{ar} + M_{al}} \quad (1)$$

$$f_{al} = \frac{M_{al}}{M_{ar} + M_{al}} \quad (2)$$

where  $M_{ar}$  and  $M_{al}$  are the fitted magnetizations of each of the two spectral regions and includes normalization of the magnetization of the aromatic region to account for magnetization appearing in spinning sidebands. The usual aromatic or  $sp^2$  region is taken from 240 to 90 ppm and includes carbonyl and carboxyl groups. The aliphatic or  $sp^3$  region is usually taken from 0 to 90 ppm. In instances when the aromatic resonance exhibits broad wings and there is not a significant amount of aliphatic carbon attached to oxygen atoms the aromatic/aliphatic cutoff may move to anywhere between 60 and 90 ppm. Each of the two main spectral regions is subdivided further into smaller regions that represent carbon atoms in more specific types of environments. This is accomplished by using the very good signal-to-noise CPMAS spectrum and scaling either  $f_a$  or  $f_{al}$  by the fraction of the total region that the subregion represents. The aromatic region is separated into the carboxyl and carbonyl region  $f_a^C$  with a chemical shift range of 240–165 ppm and the main aromatic ring region  $f_a^r$  of 165–90 ppm. The carbonyl/carboxyl region can be further subdivided into an aldehyde and ketone region,  $f_a^O$ , with a shift range of 240–185 ppm and an acid, ester, amide region,  $f_a^{OO}$ , with a shift range of 185–165 ppm. For samples where broad Lorentzian wings extend from the main aromatic band small amounts of carbonyl/carboxyl functional groups may be obscured and the parameter  $f_a^C$  is not reported.

The aromatic region can be further subdivided using the results of a dipolar dephasing experiment. This experiment determines the fraction of the aromatic ring carbons that are protonated. If  $M_G$  (magnetization that decays with Gaussian behavior) is the fraction of aromatic ring carbons with a directly attached proton, then

$$f_a^H = f_a M_G \quad (3)$$

$$f_a^N = f_a (1 - M_G) \quad (4)$$

where  $f_a^H$  represents the fraction of aromatic ring carbons with an attached proton and  $f_a^N$  represents all of the types of nonprotonated aromatic carbons. The usual integration range for the dipolar dephasing experiment is 90–165 ppm so carbonyl/carboxyl groups are not included. The nonprotonated region can be subdivided into three other regions on the basis of subintegrals. The first region  $f_a^P$ , with a chemical shift range of 150–165 ppm represents aromatic ring carbons with an attached oxygen such as phenols and phenolic ethers. The second region  $f_a^S$  represents aromatic ring carbons with an attached alkyl group and has a chemical shift range of 150–135 ppm. The parameter that represents the bridge head carbons  $f_a^B$  is given in (5)

$$f_a^B = f_a^N - f_a^P - f_a^S \quad (5)$$

Using subintegrals, the aliphatic region can also be subdivided into two regions that represent mostly methyl groups or methine plus methylene carbons. The methyl groups  $f_{al}^*$  are represented by the sum of the integral regions 0–22 ppm for methyls and 50–60 ppm for methoxy methyls. The rest of the aliphatics, methylene plus methine groups  $f_{al}^H$  are defined as

$$f_{al}^H = f_{al} - f_{al}^* \quad (6)$$

This division is probably the least precise of all the integration subregions, and some workers may want to use the dipolar dephasing experiment as described above for this separation as has been done previously.<sup>21</sup> Another subregion which overlaps some of the above two main aliphatic regions represents the total aliphatic carbon bonded to an oxygen atom  $f_{al}^O$  and covers the integral region 50–90 ppm.

The definition of the lattice parameters is based on the rather simple lattice model employed by Grant et al.<sup>30</sup> The coal structure is assumed to be represented by a distribution of macromolecular fragments. These fragments consist of aromatic clusters with side chains and bridging groups that link (with aryl–aryl, ether, or aliphatic groups) the condensed aromatic clusters.

The average aromatic cluster size  $C$  (i.e., the average number of aromatic carbon atoms per cluster) may now be calculated as has been described in ref 21 by using the mole fraction of aromatic bridgehead carbons  $\chi_b$  defined as

$$\chi_b = \frac{f_a^B}{f_a} \quad (7)$$

The relation between  $\chi_b$  and  $C$ , the average aromatic cluster size, is given as follows. For linear catenation (benzene, naphthalene, anthracene, etc.)  $\chi_b = 1/2 - 3/C$  and for circular catenation (benzene, coronene, circumcoronene, etc.)  $\chi_b = 1 - \sqrt{6}/\sqrt{C}$ . The combined model as determined in ref 21 is

(41) Hu, J. Z.; Solum, M. S.; Taylor, C. M. V.; Pugmire, R. J.; Grant, D. M. *Energy Fuels* **2001**, *15*, 14.

$$\chi_b = 1/2 \left\{ \left[ 1 - \tanh\left(\frac{C - C_0}{m}\right) \right] \chi'_b + \left[ 1 + \tanh\left(\frac{C - C_0}{m}\right) \right] \chi''_b \right\} \quad (8)$$

and where  $C_0 = 19.57$  and  $m = 4.15$ .

Another lattice parameter  $\sigma + 1$  the average number of attachments (bridges plus side chains) per cluster, is defined as follows:

$$\sigma + 1 = \frac{(f_a^P + f_a^S) \times C}{f_a} \quad (9)$$

The fraction of all possible bridges that are intact  $P_0$  is defined as

$$P_0 = \frac{f_a^P + f_a^S - f_{al}^*}{f_a^P + f_a^S} \quad (10)$$

The next two lattice parameters are B.L., the number of bridges and loops per cluster and S.C., the number of side chains per cluster. A bridge is defined as a connection between two different clusters and a loop is a bridge back to the same cluster. A side chain is an aliphatic chain attached to one cluster and assumed to end in a single methyl group. These parameters are defined as follows:

$$\text{B.L.} = P_0(\sigma + 1) \quad (11)$$

$$\text{S.C.} = (\sigma + 1) - \text{B.L.} \quad (12)$$

From elemental analysis data two additional lattice parameters may be defined. The first is MW, the average molecular weight of a cluster that is defined as follows:

$$\text{MW} = \frac{C12.01}{f_a \times \% \text{Carbon}/100} \quad (13)$$

The %carbon is taken from the elemental analysis of the coal (daf of dmmf). The last lattice parameter  $M_\delta$  is the average molecular weight of a side chain or half of a bridge mass and is defined as

$$M_\delta = \frac{\text{MW} - 13M_G C - 12(1 - M_G)C}{(\sigma + 1)} \quad (14)$$

In samples that have very broad Lorentzian wings, such as the higher temperature soots, the integral ranges described are compromised and a deconvolution of the CPMAS line shape is felt to produce more reliable results. A Fortran program written in this laboratory is used for the deconvolution fitting. Each line in the spectrum is represented by an isotropic shift, a Gaussian broadening, a Lorentzian broadening, and an integral. A simplex algorithm is used to adjust each of the parameters for each line. An example of when the deconvolution procedure is useful can be seen in the high-temperature biphenyl and pyrene samples (Figures 3 and 4) where an aliphatic peak, which represents

about 1 or 2% of the total carbon, overlaps with a broad Lorentzian wing from the large aromatic resonance. An integral range will include part of the broad wing along with the aliphatic signal that would overestimate the fraction of aliphatic material. Deconvolution of the composite line will provide a more precise value. The deconvolution procedure is not used in cases where such overlap does not occur since a unique solution cannot always be obtained for most line shapes and the relative contribution of each line varies by an unacceptable amount for each local minimum (the well has a very flat bottom). The integral ranges have been found to provide very reliable data in cases where extremes in overlap or relative intensities do not exist.

All structural data in this paper has been derived using the crosspolarization, CP, technique with the exception of one spectrum taken using the single pulse, SP, technique. Which of the two techniques is better for carbonaceous solids has been a topic of debate in the NMR community.<sup>42,43</sup> We feel that the CP procedures used in this laboratory are quite adequate, since (1) CP yields a higher signal-to-noise ratio, (2) variable contact time curves provide information on the carbonization of the sample from  $T_{1\rho}^H$  measurements i.e., time independent electron nuclear interactions (shorter  $T_{1\rho}^H$ ) vs time dependent electron nuclear interactions (conduction electrons and longer  $T_{1\rho}^H$ ), and 3) the experiment can be repeated faster due to the shorter  $T_1^H$  as compared to the much longer  $T_1^C$  needed in SP experiments. Others investigators believe that the SP technique is the more quantitative experiment.<sup>44</sup> If a sample contains carbon atoms far removed from protons then the CP technique may fail. However, it is possible to adequately polarize nonprotonated carbons "buried" in the middle of large PAH's such as pyrene,<sup>45</sup> coronene and corannulene<sup>46</sup> as demonstrated in the shift tensor data produced in this laboratory. The instability of the Hartman Hahn match (needed for CP) can, in some cases, degrade the signal from nonprotonated carbons. We have found this problem to be both probe and amplifier performance dependent and each laboratory should carefully check system stability. Background signals from fluorinated/chlorinated plastic probe or rotor components, not observed in CP experiments, may be detected in SP experiments. These background signals are not always evident against a strong signal such as hexamethylbenzene (a standard NMR setup molecule) but may distort integration values in samples with a low S/N.

EF0100294

(42) Snape, C. E.; Axelson, D. E.; Botto, R. E.; Delpuech, J. J.; Tekely, P.; Gerstein, B. C.; Pruski, M.; Maciel, G. E.; Wilson, M. A. *FUEL* **1989**, *68*, 547.

(43) Silbernagel, B. G.; Botto, R. E. In *Magnetic Resonance of Carbonaceous Solids*; Botto, R. E., Sanada, Y., Eds.; American Chemical Society: Washington, DC, 1993; Chapter 33, p 629.

(44) Maroto-Valer, M. M.; Atkinson, C. J.; Wilmers, R. R.; Snape, C. E. *Energy Fuels* **1998**, *12*, 833.

(45) Carter, C. M.; Alderman, D. W.; Facelli, J. C.; Grant, D. M. *J. Am. Chem. Soc.* **1987**, *109*, 2639.

(46) Orendt, A. M.; Facelli, J. C.; Bai, S.; Rai, A.; Gossett, M.; Scott, L. T.; Boerio-Goates, J.; Pugmire, R. J.; Grant, D. M. *J. Phys. Chem. A* **2000**, *104*, 149.